spectrum recorded after an additional 15 min gave an identical ratio.[34]

Crystal Structures. Crystals of **1b,f**$^+PF_6^-$ (above) were mounted for data collection on a Enraf-Nonius CAD-4 diffractometer as summarized in Table I. Cell constants were determined from 25 reflections with 20° < 2θ < 30° (**1b**$^+PF_6^-$) or 17° < 2θ < 25° (**1f**$^+PF_6^-$). The space groups were determined from systematic absences (**1b**$^+PF_6^-$, $h0l$ ($h + l = 2n$), $0k0$ ($k = 2n$); **1f**$^+PF_6^-$, $h0l$ ($l = 2n$), $0k0$ ($k = 2n$) and subsequent least-squares refinement. Standard reflections showed 8.1% decay during data collection for **1b**$^+PF_6^-$, but <1% for **1f**$^+PF_6^-$. Lorentz, polarization, anisotropic decay, and empirical absorption (Ψ scans) corrections were applied to the data. Intensities of equivalent reflections were averaged. The structures were solved by standard heavy-atom techniques with the SDP/VAX package.[35] Non-hydrogen atoms were refined with anisotropic thermal parameters. Hydrogen atoms were located for **1f**$^+BF_4^-$ and added to the structure factor calculations but were not refined. Scattering factors, and $\Delta f'$ and $\Delta f''$ values, were taken from the literature.[36]

Acknowledgment. We thank the NIH for support of this research and the Ministry of Education and Science of Spain and the Fulbright Commission for a postdoctoral fellowship (I.S.-L.).

Supplementary Material Available: Figure 3 (variable-temperature ^1H NMR spectra of **1i**$^+BF_4^-$ in CD_2Cl_2) and tables of anisotropic thermal parameters for **1b,f**$^+PF_6^-$ (3 pages); tables of calculated and observed structure factors (28 pages). Ordering information is given on any current masthead page.

(34) For all reactions in Scheme IV, equilibrium ratios were checked by recording additional NMR spectra at *twice* the time interval after which equilibrium appeared to be initially reached.

(35) Frenz, B. A. The Enraf-Nonius CAD 4 SDP—A Real-time System for Concurrent X-ray Data Collection and Crystal Structure Determination. In *Computing and Crystallography*; Schenk, H., Olthof-Hazelkamp, R., van Konigsveld, H., Bassi, G. C., Eds.; Delft University Press: Delft, Holland, 1978; pp 64–71.

(36) Cromer, D. T.; Waber, J. T. In *International Tables for X-ray Crystallography*; Ibers, J. A., Hamilton, W. C., Eds.; Kynoch: Birmingham, England, 1974; Vol. IV, pp 72–98, 149–150; Tables 2.2B and 2.3.1.

(37) Wiberg has recently (a) established the basicity order **f** > **i** > **c** toward the oxonium salt $(CH_3CH_2)_3O^+BF_4^-$, which parallels our data in Scheme IV and solution lability trends, and (b) conducted ab initio calculations that show the more basic C=O lone pairs in *s-trans*-methyl acetate and γ-butyrolactone correspond to those bound to rhenium in crystalline **1b,f**$^+PF_6^-$ (Figures 1 and 2). See: Wiberg, K. B.; Waldron, R. F. *J. Am. Chem. Soc.* **1991**, *113*, 7705.

Synthesis, Structure, and Reactivity of (Pentamethylcyclopentadienyl)rhenium Aldehyde Complexes $[(\eta^5\text{-}C_5Me_5)Re(NO)(PPh_3)(\eta^2\text{-}O{=}CHR)]^+BF_4^-$: Highly Diastereoselective Deuteride Additions

Francine Agbossou,† James A. Ramsden, Yo-Hsin Huang, Atta M. Arif, and J. A. Gladysz*

Department of Chemistry, University of Utah, Salt Lake City, Utah 84112

Received August 29, 1991

Reactions of the dichloromethane complex $[(\eta^5\text{-}C_5Me_5)Re(NO)(PPh_3)(ClCH_2Cl)]^+BF_4^-$ and RCH=O (R: **a**, CH_3; **b**, CH_2CH_3; **c**, $CH(CH_3)_2$; **d**, C_6H_5; **e**, $CH_2C_6H_5$) give π-aldehyde complexes (*RS,SR*)-$[(\eta^5\text{-}C_5Me_5)Re(NO)(PPh_3)(\eta^2\text{-}O{=}CHR)]^+BF_4^-$ ((*RS,SR*)-**5a–e**, 85–89%). A crystal structure of (*RS,SR*)-**5b** shows the RCH=O carbon to be anti to the PPh_3 ligand and the ethyl group to be syn to the NO ligand, confirming the stereochemical assignment. The C–O bond length (1.325 (7) Å) is intermediate between that of a single and double bond. Reactions of (*RS,SR*)-**5a–e** and formyl complex $(\eta^5\text{-}C_5H_5)Re(NO)(PPh_3)(CHO)$ (**6**) give alkoxide complexes $(\eta^5\text{-}C_5Me_5)Re(NO)(PPh_3)(OCH_2R)$ (**7a–e**, 79–88%) and $[(\eta^5\text{-}C_5H_5)Re(NO)(PPh_3)(CO)]^+BF_4^-$ (≥94%). Analogous reactions with deuterioformyl complex **6**-d_1 give **7a–e**-d_1 as 78–98:22–2 mixtures of *RR,SS* and *RS,SR* diastereomers. The mechanism of diastereoselection is analyzed. Complexes **7a–e**-d_1 epimerize at rhenium at room temperature.

The conversion of achiral aldehydes to enantiomerically pure alcohol derivatives is a major objective of asymmetric organic synthesis.[1] Accordingly, many chiral, optically active transition-metal compounds are now available[2] and would appear to have considerable untapped potential for effecting enantioselective nucleophilic additions in both catalytic and stoichiometric modes.

We have found that the chiral rhenium dichloromethane complex $[(\eta^5\text{-}C_5H_5)Re(NO)(PPh_3)(ClCH_2Cl)]^+BF_4^-$ is easily generated in enantiomerically pure form and serves as a functional equivalent of the chiral Lewis acid $[(\eta^5\text{-}C_5H_5)Re(NO)(PPh_3)]^+$ (I).[3] This pyramidal fragment is a powerful π donor and possesses the d-orbital HOMO shown in Figure 1. Hence, aldehydes react to give π complexes $[(\eta^5\text{-}C_5H_5)Re(NO)(PPh_3)(\eta^2\text{-}O{=}CHR)]^+BF_4^-$ (1) with structures IIa and IIIa.[4,5] In each case, the substituted =CHR terminus is oriented anti to the bulky PPh_3 ligand. Adducts IIa and IIIa are diastereomeric and differ in the aldehyde enantioface bound to rhenium. Note that the aldehyde substituent is directed at the small nitrosyl ligand in IIa and the larger cyclopentadienyl ligand in IIIa.

† Formerly Francine Niedercorn.

(1) Some lead references: (a) Kitamura, M.; Okada, S.; Suga, S.; Noyori, R. *J. Am. Chem. Soc.* **1989**, *111*, 4028. (b) Togni, A.; Pastor, S. D. *J. Org. Chem.* **1990**, *55*, 1649. (c) Duthaler, R. O.; Hafner, A.; Riediker, M. In *Organic Synthesis via Organometallics*; Dötz, K. H., Hoffmann, R. W. Eds.; Vieweg: Braunschweig, Germany, 1991; pp 285–309.

(2) See articles published in: Organometallic Compounds and Optical Activity. *J. Organomet. Chem.* **1989**, *370* (Brunner, H., Volume Ed.).

(3) Fernández, J. M.; Gladysz, J. A. *Organometallics* **1989**, *8*, 207.

(4) Garner, C. M.; Quirós Mendez, N.; Kowalczyk, J. J.; Fernández, J. M.; Emerson, K.; Larsen, R. D.; Gladysz, J. A., *J. Am. Chem. Soc.* **1990**, *112*, 5146.

(5) Quirós Méndez, N.; Mayne, C. L.; Gladysz, J. A. *Angew. Chem., Int. Ed. Engl.* **1990**, *29*, 1475.

0276-7333/92/2311-0693$03.00/0

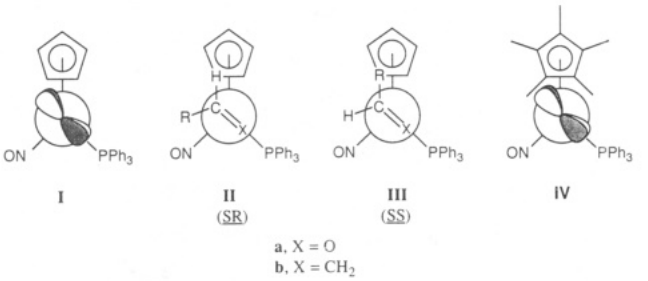

Figure 1. Key: I, pyramidal rhenium fragment $[(\eta^5\text{-}C_5H_5)Re(NO)(PPh_3)]^+$ with d-orbital HOMO; II and III, Newman projections of possible diastereomers of aldehyde and alkene complexes $[(\eta^5\text{-}C_5H_5)Re(NO)(PPh_3)(\eta^2\text{-}X{=}CHR)]^+$; IV, pyramidal fragment $[(\eta^5\text{-}C_5Me_5)Re(NO)(PPh_3)]^+$ with d-orbital HOMO.

Accordingly, aliphatic and aromatic aldehydes exhibit binding selectivities of ≥99:1 and 98–81:2–19, respectively.[5] Nucleophiles readily add to the aldehyde carbon to give alkoxide complexes $(\eta^5\text{-}C_5H_5)Re(NO)(PPh_3)(OCH(Nu)R)$ (**2**) as >98–75:2–25 mixtures of diastereomers.[4,6]

In all cases, the stereochemistry of the major diastereomers of alkoxide complexes **2** is consistent with that expected from nucleophilic attack upon IIa from a direction anti to the rhenium. However, the addition diastereoselectivities are generally lower than enantioface binding selectivities. This suggests a potentially complex mechanism of diastereoselection. Several relevant observations have been made. First, the interconversion of IIa and IIIa has been shown (1) to be rapid below room temperature, (2) to be intramolecular, and (3) to involve intermediate σ complexes.[5] Second, monosubstituted alkenes can be considered "isosteric" to aldehydes and bind in a similar fashion to I, as depicted in IIb and IIIb (Figure 1).[7] However, diastereomers IIb and IIIb are separable—equilibration to 95–99:5–1 IIb/IIIb mixtures occurs only at 95–100 °C.[7,8] Also, nucleophiles attack each alkene complex diastereomer stereospecifically (≥99:1) upon the π face anti to the rhenium.[9]

In order to improve the diastereoselectivity of nucleophilic additions to aldehyde complexes **1**, we have sought to define the origin of the minor diastereomers of alkoxide complexes **2**. Among other possibilities, we have considered mechanisms involving attack upon the small equilibrium quantitites of (1) IIIa or (2) isomeric σ complexes. In any case, IIa would have to be less reactive than an alternative isomer to account for the product ratios. It is also possible that *both* diastereomers of **2** form via σ complexes. For example, σ complexes of methyl ketones, $[(\eta^5\text{-}C_5H_5)Re(NO)(PPh_3)(\eta^1\text{-}O{=}C(CH_3)R)]^+X^-$, similarly undergo highly diastereoselective nucleophilic additions.[6b,10] Furthermore, complexes of I and certain substituted benzaldehydes exist predominantly as σ isomers.[11]

As part of several independent probes of the preceding possibilities, we decided to study the reactivity of analogous *pentamethyl*cyclopentadienyl complexes. The corresponding Lewis acid fragment $[(\eta^5\text{-}C_5Me_5)Re(NO)(PPh_3)]^+$ (IV) has a comparable d-orbital HOMO (Figure 1) and should be an even stronger π donor.[12,13] This, coupled with the increased bulk of the substituted cyclopentadienyl ligand should give higher equilibrium ratios of π diastereomers of the types IIa and IIIa. Thus, higher addition diastereoselectivities should be observed if diastereoselection is controlled by attack upon π isomers. In this paper, we report (1) high-yield syntheses of aldehyde complexes $[(\eta^5\text{-}C_5Me_5)Re(NO)(PPh_3)(\eta^2\text{-}O{=}CHR)]^+BF_4^-$, (2) a crystal structure of a propionaldehyde complex, (3) the highly diastereoselective addition of deuteride to these complexes, and (4) an analysis of the mechanism of diastereoselection.

Scheme I. Syntheses of Aldehyde Complexes $(RS,SR)\text{-}[(\eta^5\text{-}C_5Me_5)Re(NO)(PPh_3)(\eta^2\text{-}O{=}CHR)]^+BF_4^-$ ((*RS*,*SR*)-5)

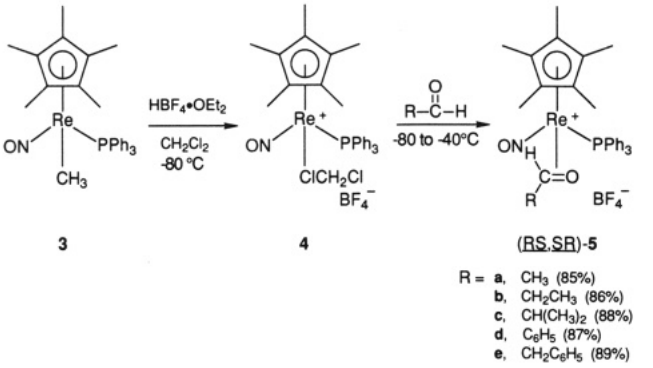

Results

1. Synthesis of Aldehyde Complexes. The pentamethylcyclopentadienyl methyl complex $(\eta^5\text{-}C_5Me_5)Re(NO)(PPh_3)(CH_3)$ (**3**) and $HBF_4{\cdot}OEt_2$ were combined in CH_2Cl_2 at −80 °C as previously described to give the dichloromethane complex $[(\eta^5\text{-}C_5Me_5)Re(NO)(PPh_3)(ClCH_2Cl)]^+BF_4^-$ (**4**).[14] Then 3 equiv of (**a**) acetaldehyde, (**b**) propionaldehyde, (**c**) isobutyraldehyde, (**d**) benzaldehyde, and (**e**) phenylacetaldehyde were added. Workup gave the π-aldehyde complexes $(RS,SR)\text{-}[(\eta^5\text{-}C_5Me_5)Re(NO)(PPh_3)(\eta^2\text{-}O{=}CHR)]^+BF_4^-$ ((*RS*,*SR*)-**5a–e**)[15] in 85–89% yields as amber (**5a–c,e**) to pink (**5d**) powders (Scheme I).

The reaction of **4** and benzaldehyde was monitored by ^{31}P NMR spectroscopy. Complex (*RS*,*SR*)-**5d** formed in quantitative yield over the course of 2 h at −40 °C. Product stereochemistry was assumed to be analogous to that of the corresponding cyclopentadienyl complexes **1**. This was confirmed crystallographically, as described below.

Complexes (*RS*,*SR*)-**5a–e** were characterized by microanalysis (Experimental Section) and by IR and NMR (^1H, ^{13}C, ^{31}P) spectroscopy (Table I). The IR ν_{NO} values (1707–1710 cm^{-1}, KBr) were similar to those of other cationic complexes, $[(\eta^5\text{-}C_5Me_5)Re(NO)(PPh_3)(L)]^+X^-$.[14,16] However, they were 27–39 cm^{-1} *lower* than for cyclo-

(6) (a) Garner, C. M.; Fernández, J. M.; Gladysz, J. A. *Tetrahedron Lett.* **1989**, *30*, 3931. (b) Dalton, D. M.; Garner, C. M.; Fernández, J. M.; Gladysz, J. A. *J. Org. Chem.* **1991**, *56*, 6823.

(7) (a) Bodner, G. S.; Fernández, J. M.; Arif, A. M.; Gladysz, J. A. *J. Am. Chem. Soc.* **1988**, *110*, 4082. (b) Bodner, G. S.; Peng, T.-S.; Arif, A. M.; Gladysz, J. A. *Organometallics* **1990**, *9*, 1191. (c) Peng, T.-S.; Arif, A. M.; Gladysz, J. A. *Helv. Chim. Acta*, in press.

(8) (a) Peng, T.-S.; Gladysz, J. A. *J. Chem. Soc., Chem. Commun.* **1990**, 902. (b) Peng, T.-S.; Gladysz, J. A. Submitted for publication.

(9) (a) Peng, T.-S.; Gladysz, J. A. *Tetrahedron Lett.* **1990**, *31*, 4417. (b) Peng, T.-S. Ph.D. Thesis, University of Utah, 1991.

(10) Dalton, D. M.; Fernández, J. M.; Emerson, K.; Larsen, R. D.; Arif, A. M.; Gladysz, J. A. *J. Am. Chem. Soc.* **1990**, *112*, 9198.

(11) Quirós Méndez, N.; Arif, A. M.; Gladysz, J. A. *Angew. Chem., Int. Ed. Engl.* **1990**, *29*, 1473.

(12) Lichtenberger, D. L.; Rai-Chaudhuri, A.; Seidel, M. J.; Gladysz, J. A.; Agbossou, S. K.; Igau, A.; Winter, C. H. *Organometallics* **1991**, *10*, 1355.

(13) (a) Lichtenberger, D. L.; Kellog, G. E. *Acc. Chem. Res.* **1987**, *20*, 379. (b) Elschenbroich, C.; Salzer, A. *Organometallics*; VCH: New York, 1989; p 47. (c) Sowa, J. R., Jr.; Angelici, R. J. *J. Am. Chem. Soc.* **1991**, *113*, 2537.

(14) Winter, C. H.; Gladysz, J. A. *J. Organomet. Chem.* **1988**, *354*, C33.

(15) The absolute configuration at rhenium (the higher priority atom) is specified first. Rhenium and carbon configurations are assigned as previously described.[4]

(16) Patton, A. T.; Strouse, C. E.; Knobler, C. B.; Gladysz, J. A. *J. Am. Chem. Soc.* **1983**, *105*, 5804.

pentadienyl analogues 1,[4] reflecting the greater π basicity of the pentamethylcyclopentadienyl fragment IV.[12,13] The ^{1}H NMR chemical shifts of the aldehyde protons in the aliphatic complexes (*RS,SR*)-**5a–c,e** (δ 4.0–4.4) were upfield of that of the benzaldehyde complex (*RS,SR*)-**5d** (δ 5.63). All of these were in turn ≥1 ppm upfield of the aldehyde proton resonances in 1. The ^{31}P NMR chemical shifts (7.8–9.5 ppm) were also slightly upfield of those of 1 (10.0–10.1 ppm). However, the ^{13}C NMR chemical shifts of the aldehydic carbons (80–93 ppm) were quite similar in both classes of compounds.

Solutions of benzaldehyde complex (*RS,SR*)-**5d** were red-violet at room temperature, but honey yellow at −80 °C. Solutions of the aliphatic aldehyde complexes (*RS, SR*)-**5a–c,e** did not exhibit noticeable thermochromism. It has been previously shown that σ isomers of analogous cyclopentadienyl aromatic aldehyde complexes are deep red and that π to σ ratios increase upon cooling.[11] Also, σ isomers give IR ν_{NO} that are ca. 40 cm^{-1} lower than those of π isomers.[11] No trace of a second ν_{NO} was found for (*RS,SR*)-**5a–c,e** in solution or the solid state. However, (*RS,SR*)-**5d** exhibited two ν_{NO} at 1719 (vs) and 1684 (w) cm^{-1} in CH_2Cl_2 at 26 °C. The relative areas of the absorbtions indicated a π to σ ratio of (78 ± 2):(22 ± 2).[11]

Both ^{1}H and ^{31}P NMR spectra of (*RS,SR*)-**5d** were recorded at low temperatures. No evidence was found for the decoalescence of π and σ isomers, or *RS,SR* and *RR,SS* π diastereomers, in CD_2Cl_2 at −100 °C or $CDFCl_2$ at −145 °C. Chemical shifts for these species can be confidently predicted from earlier work.[5] However, one unexplained phenomenon was observed. At −110 °C, the benzaldehyde proton ^{1}H NMR resonance decoalesced into two resonances of essentially equal intensity. Limiting low-temperature data were as follows (500 MHz): −135 °C, δ 6.80/4.75, $\Delta\nu$ 1038.1 Hz; −145 °C, δ 6.82/4.70, $\Delta\nu$ 1060.1 Hz, (53 ± 2):(47 ± 2).[17] Application of the coalescence formula gave a $\Delta G^{\ddagger}$(−110 °C) of 6.8 ± 0.1 kcal/mol for the dynamic process that interconverts the two species.[17c] The nature of the isomers responsible for this behavior remains under investigation.

Attempts were made to similarly convert the optically active methyl complex (+)-(*S*)-**3**[18,19] to optically active aldehyde complexes (+)-(*RS*)-**5**. The resulting powders were more soluble than the racemates and could not in our hands be isolated in analytically pure form. However, optical rotations were appreciable. In another approach, (+)-(*S*)-**3** was treated with $HBF_4{\cdot}OEt_2$ in chlorobenzene. Based upon precedent in the cyclopentadienyl series,[20] a labile chlorobenezene complex is likely generated. Subsequent addition of isobutyraldehyde and workup gave (+)-(*RS*)-**5c**, $[\alpha]^{25}_{589}$ 112°, that was not quite analytically pure. Finally, the chiral NMR shift reagents (+)-Eu(hfc)$_3$ and (+)-Pr(hfc)$_3$ (3–4 equiv, CD_2Cl_2) did not resolve the pentamethylcyclopentadienyl ^{1}H NMR resonances of the enantiomers of racemic (*RS,SR*)-**5a,d** (0.3–0.5 M).

2. Crystal Structure of Propionaldehyde Complex (*RS,SR*)-5b. X-ray data were acquired on crystals of (*RS,SR*)-**5b** as outlined in Table II. Refinement, described in the Experimental Section, yielded the structures shown in Figure 2. Atomic coordinates and key bond lengths and angles are summarized in Tables III and IV. Anisotropic thermal parameters and structure factors are given in the supplementary material. Figure 2 shows that the complex crystallizes as a *RS,SR* diastereomer (IIa, Figure 1).

Additional structural properties were calculated. The Re–C29–O2 plane made 22.8° and 66.8° angles with the

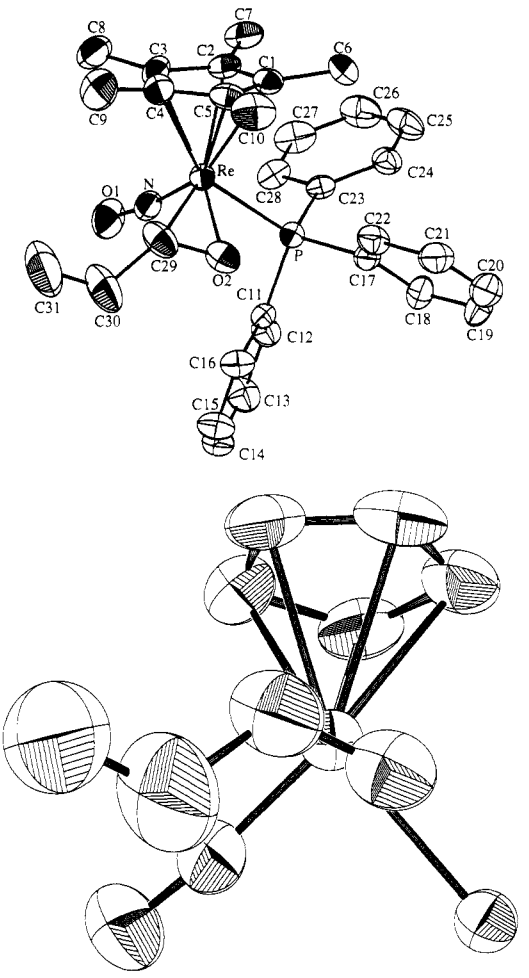

Figure 2. Structure of the cation of propionaldehyde complex (*RS,SR*)-[(η^5-C_5Me_5)Re(NO)(PPh_3)(η^2-O=$CHCH_2CH_3$)]$^+BF_4^-$ ((*RS,SR*)-**5b**): top, numbering diagram; bottom, Newman-type projection with phenyl rings and cyclopentadienyl methyl groups omitted.

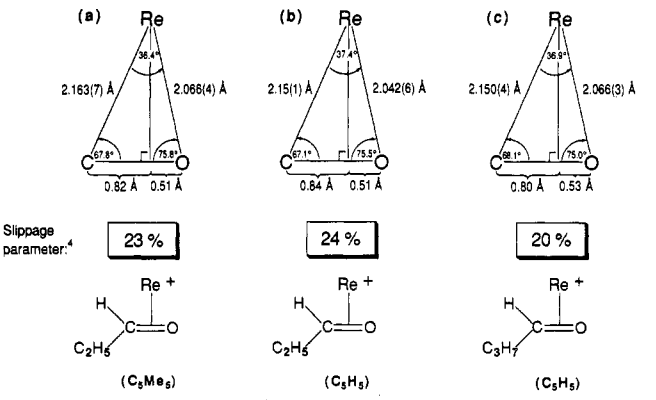

Figure 3. Views of the Re–C–O planes: (a) propionaldehyde complex (*RS,SR*)-**5b**, (b) propionaldehyde complex (*RS,SR*)-[(η^5-C_5H_5)Re(NO)(PPh_3)(η^2-O=$CHCH_2CH_3$)]$^+PF_6^-$ ((*RS,SR*)-**10**),[28] (c) butyraldehyde complex (*RS,SR*)-[(η^5-C_5H_5)Re(NO)(PPh_3)(η^2-O=$CHCH_2CH_2CH_3$)]$^+PF_6^-$ ((*RS,SR*)-**11**).[28]

(17) (a) Chemical shifts were referenced to residual $CHFCl_2$ (δ 7.47): Siegel, J. S.; Anet, F. A. L. *J. Org. Chem.* **1988**, *53*, 2629. (b) Probe temperatures were calibrated with methanol and are considered accurate to ±1 °C. (c) Sandström, J. *Dynamic NMR Spectroscopy*; Academic Press: New York, 1982; Chapter 7. The error limit assumes that T_{coal} is accurate to ±2 °C.

(18) Prefixes (+) and (−) refer to rotations at 589 nm. All rotations were measured in thermostated cells.

(19) Huang, Y.-H.; Niedercorn, F.; Arif, A. M.; Gladysz, J. A. *J. Organomet. Chem.* **1990**, *383*, 213.

(20) Kowalczyk, J. J.; Agbossou, S. K.; Gladysz, J. A. *J. Organomet. Chem.* **1990**, *397*, 333.

Scheme II. Syntheses of Alkoxide Complexes (η^5-C_5Me_5)Re(NO)(PPh_3)(OCH_2R) (7)

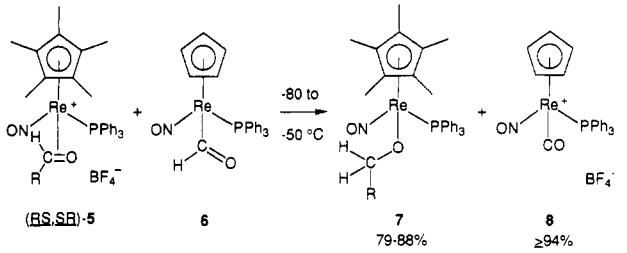

Re–PPh_3 and Re–NO bonds, respectively. These deviate somewhat from the corresponding 0° and 90° angles in the idealized structure IIa. Also, the C29–C30 bond was bent out of the π nodal plane of the free aldehyde. In order to quantify this feature, a plane was defined that contained C29 and O2 but was perpendicular to the Re–C29–O2 plane. The angle of the C29–C30 bond with this plane was 21°. In the free aldehyde, the analogous angle would be 0°. Finally, the Re–C29–O2 moiety was distorted or "slipped", with the rhenium significantly closer to oxygen than carbon, as shown in Figure 3a.

3. Synthesis of Alkoxide Complexes. The formyl complex (η^5-C_5H_5)Re(NO)(PPh_3)(CHO) (**6**)[21] efficiently reduces cyclopentadienyl aldehyde complexes **1** to the corresponding alkoxide complexes between −80 and −60 °C.[4] Hence, (*RS,SR*)-**5a–e** and **6** were combined in CH_2Cl_2 at −80 °C (Scheme II). Workup gave the alkoxide complexes (η^5-C_5Me_5)Re(NO)(PPh_3)(OCH_2R) (**7a–e**) and carbonyl complex [(η^5-C_5H_5)Re(NO)(PPh_3)(CO)]$^+BF_4^-$ (**8**) in 79–88% and ≥94% yields, respectively. Separate NMR experiments showed the reactions to be spectroscopically quantitative and to proceed over the temperature range of −80 to −50 °C.

The alkoxide complexes **7a–e** were obtained as tan-red foams, which were characterized analogously to (*RS, SR*)-**5a–e**. Data are summarized in Table I and the Experimental Section. The IR ν_{NO} (1606–1623 cm^{-1}) resembled those of other neutral (η^5-C_5Me_5)Re(NO)(PPh_3)(X) complexes.[12,16,22,23] Interestingly, values were usually slightly *higher* than those of the cyclopentadienyl analogues (η^5-C_5H_5)Re(NO)(PPh_3)(OCH_2R).[4] Importantly, the ^1H NMR resonances of the diastereotopic OCH_2 methylene hydrogens were in each case well-separated, as illustrated in the bottom spectrum in Figure 4.

Next, (*RS,SR*)-**5a–e** and the deuterioformyl complex (η^5-C_5H_5)Re(NO)(PPh_3)(CDO) (**6**-d_1)[4] were combined in CD_2Cl_2 at −80 °C (Scheme III). Reactions were monitored by ^1H NMR spectroscopy, and spectra of the type shown in Figure 4 were acquired for each substrate. Reduction occurred with high diastereoselectivity to give the deuterated alkoxide complexes (*RR,SS*)-(η^5-C_5Me_5)Re(NO)-(PPh_3)(OCHDR) ((*RR,SS*)-**7a–e**-d_1). Stereochemistry was assigned by analogy to the corresponding reactions of the cyclopentadienyl aldehyde complexes **1**.[4]

When samples of (*RR,SS*)-**7a–e**-d_1 were warmed above 0 °C, some epimerization was detectable (Figure 4). Similar configurational instability has been observed with secondary alkoxide complexes (η^5-C_5R_5)Re(NO)(PPh_3)-(OCHRR′). A detailed study, which establishes initial epimerization at rhenium, has recently been completed.[23] The mechanism involves PPh_3 dissociation, with anchimeric assistance of the alkoxide ligand lone pair, to give the

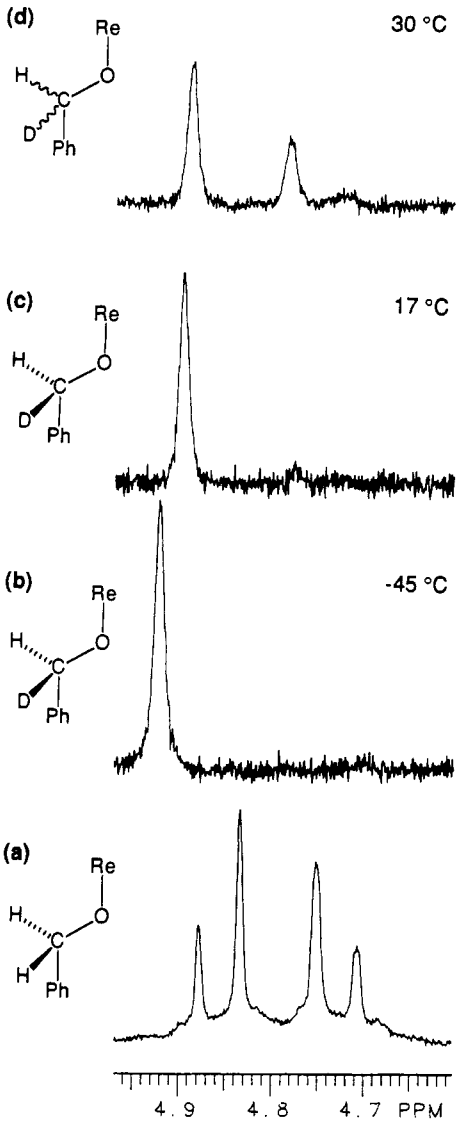

Figure 4. Representative ^1H NMR spectra of the OCH_2/OCHD protons of alkoxide complexes **7d**-d_x: (a) (η^5-C_5Me_5)Re(NO)-(PPh_3)($OCH_2C_6H_5$) (**7d**); (b) (*RR,SS*)-**7d**-d_1 at −45 °C (Scheme III); (c) the preceding sample upon warming to 17 °C; (d) the preceding sample after a period at 30 °C.

Scheme III. Deuteride Reduction of Aldehyde Complexes (*RS,SR*)-5 (Reactants and Products Are Racemic)

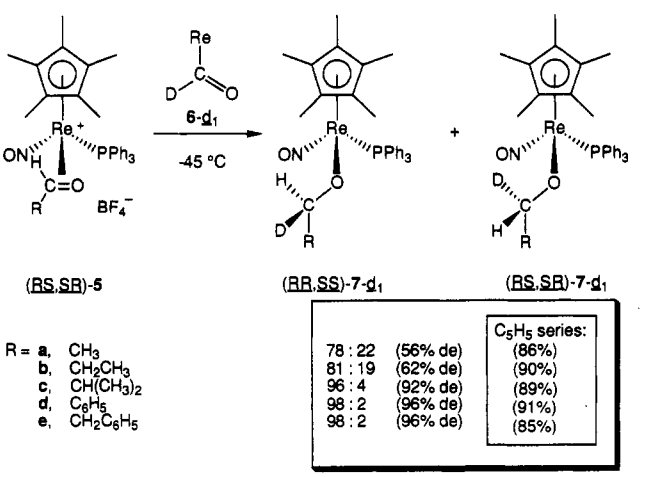

(21) Tam, W.; Lin, G.-Y.; Wong, W.-K.; Kiel, W. A.; Wong, V. K.; Gladysz, J. A. *J. Am. Chem. Soc.* **1982**, *104*, 141.
(22) (a) Heah, P. C.; Patton, A. T.; Gladysz, J. A. *J. Am. Chem. Soc.* **1986**, *108*, 1185. (b) Crocco, G. L.; Gladysz, J. A. *Ibid.* **1988**, *110*, 6110.
(23) (a) Saura-Llamas, I.; Garner, C. M.; Gladysz, J. A. *Organometallics* **1991**, *10*, 2533. (b) Saura-Llamas, I.; Gladysz, J. A. *J. Am. Chem. Soc.*, in press.

Scheme IV. Comparison of π/σ Equilibria in Cyclopentadienylrhenium Complexes

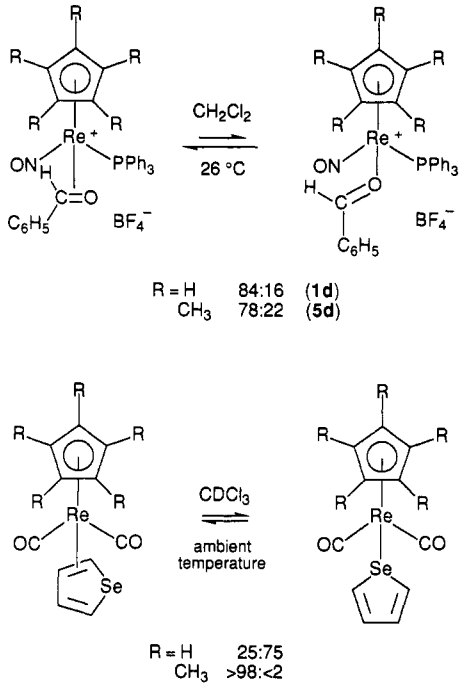

trigonal-planar alkoxide complex **9** shown in eq i. This process occurs much more readily in pentamethylcyclopentadienyl complexes.

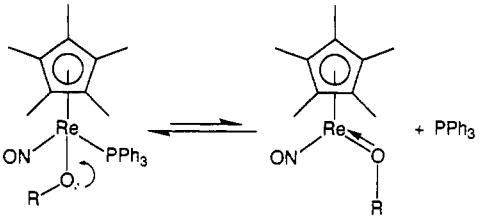

(i)

9

Finally, the optically active isobutyraldehyde complex (+)-(*RS*)-**5c** and **6** were similarly reacted. The resulting alkoxide complex (+)-(*R*)-**7c** could not be isolated in analytically pure form. However, the optical rotation of the crude material (e.g., 29 ± 4°) dropped to 0° over the course of 1–2 h in CH_2Cl_2 at room temperature. An identical result was obtained upon attempted synthesis of the optically active ethoxide complex (+)-(*R*)-**7a** from (+)-(*RS*)-**5a**. These data further substantiate the configurational instability of **7** at rhenium.

Discussion

1. Structures of Aldehyde Complexes. The availability of cyclopentadienyl and pentamethylcyclopentadienyl aldehyde complexes **1** and **5** allows a detailed comparison of the binding properties of fragments I and IV (Figure 1). First, consider π/σ equilibria (Scheme IV). Adducts of I and aliphatic aldehydes do not give detectable quantities of σ isomers in CH_2Cl_2 at 26 °C. However, the benzaldehyde complex **1d** exists as a 84:16 mixture of π/σ isomers.[11] The greater π basicity of IV should lead to enhanced π to σ ratios on electronic grounds.[12,13] However, π isomers increase congestion about the metal, and thus an opposite trend would be expected on steric grounds. In actuality, the pentamethylcyclopentadienyl benzaldehyde complex **5d** exhibits a comparable π to σ isomer ratio (78:22), indicating that these two effects approximately cancel.

In relevant related work, Angelici has studied π/σ equilibria in selenophene complexes of neutral $(\eta^5\text{-}C_5R_5)\text{-}Re(CO)_2$ fragments.[24] He finds that π to σ ratios for pentamethylcyclopentadienyl complexes are significantly higher than for cyclopentadienyl complexes, as illustrated in Scheme IV. The diminished bulk of the rhenium ligands relative to those in I and IV likely accounts for this difference.

The aldehyde enantioface binding selectivities of I and IV cannot, unfortunately, be quantitatively compared. The cyclopentadienyl benzaldehyde complex **1d** exists as a (85 ± 2):(15 ± 2) mixture of *RS,SR*/*RR,SS* diastereomers (IIa/IIIa), as assayed by low-temperature ^1H, ^{13}C, and ^{31}P NMR spectroscopy.[5] Our inability to decoalesce analogous isomers of **5d** under much more extreme temperature conditions suggests a much higher equilibrium ratio, consistent with intuitive expectations. However, differences will likely have to be modeled by measurements with the corresponding monosubstituted alkene complexes, for which diastereomer interconversion is slower.

Next, consider the geometric features of the Re–C–O moiety in propionaldehyde complex (*RS,SR*)-**5b** (Figure 3). A crystal structure of the cyclopentadienyl analogue (*RS,SR*)-**1b** has been previously reported.[4] However, the ethyl group was disordered, decreasing the reliability of the metrical parameters. Hence, we recently determined the crystal structures of the corresponding hexafluorophosphate salt (*RS,SR*)-$[(\eta^5\text{-}C_5H_5)Re(NO)(PPh_3)(\eta^2\text{-}O{=}CHCH_2CH_3)]^+PF_6^-$ ((*RS,SR*)-**10**) and the butyraldehyde complex (*RS,SR*)-$[(\eta^5\text{-}C_5H_5)Re(NO)(PPh_3)(\eta^2\text{-}O{=}CHCH_2CH_2CH_3)]^+PF_6^-$ ((*RS,SR*)-**11**).[25] The latter was determined at low temperature and is of somewhat better quality. Data are summarized in Figure 3.

First, the C⋯O bond lengths of (*RS,SR*)-**5b**, (*RS,SR*)-**10**, and (*RS,SR*)-**11** (1.325 (7), 1.35 (1), 1.338 (5) Å) are identical within experimental error. As expected, they are considerably longer than the C=O bond in propionaldehyde (1.209 (4) Å)[26] but shorter than the C—O bond in 1-propanol (1.41 Å).[27] Second, all three complexes exhibit similar rhenium–carbon and rhenium–oxygen bond lengths (Figure 3). Thus, the carbon π termini are "slipped" away from the rhenium by comparable amounts. Third, the angles of the $\overline{\text{Re-C-O}}$ planes with the Re–P bonds (22.8°, 20.2°, 20.5°) and Re–N bonds (66.8°, 73.0°, 69.5°) are also quite close. Thus, (*RS,SR*)-**5b** exhibits only a slightly greater deviation from the idealized Re–(C⋯O) conformation in IIa than (*RS,SR*)-**10** and (*RS,SR*)-**11**.

2. Deuteride Reduction of Aldehyde Complexes. As summarized in Scheme III, the diastereoselectivities for deuteride reduction of (*RS,SR*)-**5** are similar to those found earlier for cyclopentadienyl complexes **1**. Values for acetaldehyde and propionaldehyde complexes (*RS,RS*)-**5a,b** are lower, whereas values for benzaldehyde and phenylacetaldehyde complexes (*RS,SR*)-**5d,e** are higher. Regardless, the data are not consistent with a mechanism in which diastereoselection is governed by the relative quantities of π isomers IIa and IIIa. Otherwise, higher diastereoselectivities should have been obtained in the pentamethylcyclopentadienyl series.

Thus, we presently favor mechanisms involving nucleophilic addition to σ isomers—for which *E* and *Z* C=O geometric isomers would be possible. Based upon extensive studies of the corresponding methyl ketone com-

(24) Choi, M.-G.; Angelici, R. J. *J. Am. Chem. Soc.* **1991**, *113*, 5651.
(25) Klein, D. P.; Arif, A. M. Unpublished results, University of Utah.
(26) van Nuffel, P.; van den Enden, L.; van Alsenoy, C.; Geise, H. J. *J. Mol. Struct.* **1984**, *116*, 99.
(27) Aziz, N. E. A.; Rogowski, F. *Z. Naturforsch.* **1964**, *19b*, 967.

Table I. Spectroscopic Characterization of New Rhenium Aldehyde and Alkoxide Complexes

complex	IR (ν_{NO}, cm^{-1})	^1H NMR (δ)[a]	$^{13}C\{^1H\}$ NMR (ppm)[b]	$^{31}P\{^1H\}$ NMR (ppm)[c]
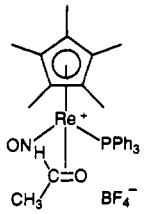 (*RS,SR*)-**5a**	1710 vs (KBr) 1719 vs (CH_2Cl_2)	7.68–7.46 (m, 3 C_6H_5), 4.44 (m, HCO), 2.12 (dd, J_{HH} = 4.0, J_{HP} = 0.8, CH_3), 1.82 (d, J_{HP} = 1.0, $C_5(CH_3)_5$)	PPh_3 at[d] 133.9 (d, J = 9.0, o), 133.0 (s, p), 129.7 (d, J = 11.0, m); 109.4 (s, $C_5(CH_3)_5$), 80.0 (s, HCO),[e] 23.5 (s, CH_3), 10.0 (s, $C_5(CH_3)_5$)	8.9 (s)
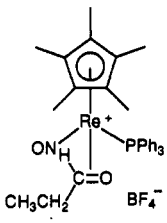 (*RS,SR*)-**5b**	1708 vs (KBr) 1719 vs (CH_2Cl_2)	7.66–7.47 (m, 3 C_6H_5), 4.32 (pseudo dt, J_{HH} = 4.6, J_{HP} = 3.3, HCO), 2.57 (dddq, J_{HH} = 15.7, 7.5, 4.6, J_{HP} = 1.2, CHH′), 1.83 (d, J_{HP} = 1.0, $C_5(CH_3)_5$), 1.63 (ddq, J_{HH} = 14.6, 7.5, 5.4, CHH′), 1.13 (t, J_{HH} = 7.5, CH_3)	PPh_3 at[d] 133.9 (br s, o), 132.9 (s, p), 129.7 (d, J = 11.0, m); 109.4 (s, $C_5(CH_3)_5$), 89.3 (br s, HCO), 31.8 (s, CH_2), 12.7 (s, CH_3), 10.2 (s, $C_5(CH_3)_5$)	8.3 (s)
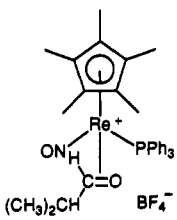 (*RS,SR*)-**5c**	1707 vs (KBr) 1717 vs (CH_2Cl_2)	7.68–7.45 (m, 3 C_6H_5), 4.05 (m, HCO), 1.84 (d, J_{HP} = 1.0, $C_5(CH_3)_5$), 1.23 (m, CHCH_3), 0.99 (m, CHC′H_3)[f]	PPh_3 at[d] 134.0 (br s, o), 133.0 (s, p), 129.6 (d, J = 11.4, m); 109.5 (s, $C_5(CH_3)_5$), 93.4 (br s, HCO), 37.9 (s, CH), 25.2 (s, $CHCH_3$), 18.1 (s, CHC′H_3), 10.3 (s, $C_5(CH_3)_5$)	7.8 (s)
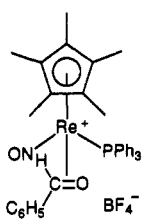 (*RS,SR*)-**5d**	1707 vs (KBr) 1720 vs 1681 w (CH_2Cl_2)	7.72–7.50 (m, 3 PC_6H_5), 7.16–7.10 and 6.50–6.44 (m, CC_6H_5), 5.63 (br s, HCO), 1.85 (s, $C_5(CH_3)_5$)	PPh_3 at[d] 134.3 (d, J = 10.0, o), 132.9 (d, J = 3.0, p), 129.8 (d, J = 11.0, m); CPh at 139.4 (s, i), 130.4 (s, p), 128.4 (s), 126.1 (s); 109.4 (s, $C_5(CH_3)_5$), 80.0 (br s, HCO), 10.4 (s, $C_5(CH_3)_5$)	9.5 (s)
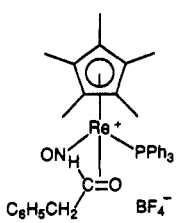 (*RS,SR*)-**5e**	1709 vs (KBr) 1718 vs (CH_2Cl_2)	7.70–7.50 (m, 3 PC_6H_5), 7.44–7.42 and 7.22–7.18 (m, CC_6H_5), 4.35 (m, HCO), 3.80 (dd, J_{HH} = 14.2, 3.9, CHH′), 2.92 (dd, J_{HH} = 14.3, 5.2, CHH′), 1.69 (s, $C_5(CH_3)_5$)	PPh_3 at[d,g] 129.6 (d, J = 11.0, o), 123.3 (d, J = 12.0, m); CPh at 137.6 (s), 127.6 (s); 109.8 (s, $C_5(CH_3)_5$), 84.2 (s, HCO),[e] 44.9 (s, CH_2), 10.1 (s, $C_5(CH_3)_5$)	8.9 (s)
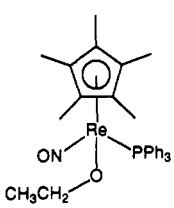 **7a**	1611 vs (film) 1611 vs (KBr)	7.83–7.77 (m, 6 H of 3 C_6H_5), 7.15–6.98 (m, 9 H of 3 C_6H_5), 4.19 (dq, J_{HH} = 9.9, 6.9, CHH′), 3.99 (dq, J_{HH} = 9.8, 6.8, CHH′), 1.59 (s, $C_5(CH_3)_5$), 1.10 (t, J_{HH} = 6.8, CH_2CH_3)	PPh_3 at 134.9 (d, J = 47.0, i), 134.6 (d, J = 10.1, o), 129.6 (s, p), 127.9 (d, J = 9.7, m); 99.7 (s, $C_5(CH_3)_5$), 77.3 (d, J = 5.7, CH_2), 22.6 (s, CH_2CH_3), 10.5 (s, $C_5(CH_3)_5$)	16.2 (s)
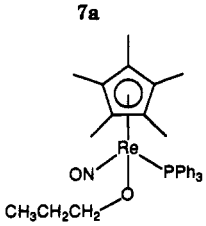 **7b**	1612 vs (film) 1606 vs (KBr)	7.83–7.76 (m, 6 H of 3 C_6H_5), 7.08–7.00 (m, 9 H of 3 C_6H_5), 4.01 (br t, J_{HH} = 6.2, OCH_2),[h] 1.60 (s, $C_5(CH_3)_5$), 1.49 (m, CCH_2C), 0.88 (t, J_{HH} = 7.3, CH_2CH_3)	PPh_3 at 135.1 (d, J = 46.8, i), 134.5 (d, J = 10.3, o), 129.6 (s, p), 128.0 (d, J = 9.9, m); 99.6 (s, $C_5(CH_3)_5$), 84.5 (d, J = 5.7, OCH_2), 30.3 (s, CCH_2C), 11.4 (s, CH_2CH_3), 10.5 (s, $C_5(CH_3)_5$)	16.6 (s)

Table I (Continued)

complex	IR (ν_{NO}, cm^{-1})	^{1}H NMR (δ)[a]	^{13}C{^{1}H} NMR (ppm)[b]	^{31}P{^{1}H} NMR (ppm)[c]
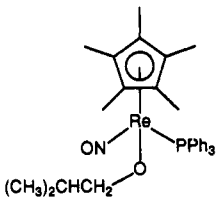 7c	1611 vs (film) 1612 vs (KBr)	7.78–7.75 (m, 6 H of 3 C_6H_5), 7.07–7.00 (m, 9 H of 3 C_6H_5), 3.90 (dd, J_{HH} = 9.1, 6.4, OC*H*H′), 3.75 (dd, J_{HH} = 9.3, 6.6, OCH*H*′), 1.60 (s, $C_5(CH_3)_5$), 0.92 (d, J_{HH} = 6.7, CHC*H*$_3$), 0.83 (d, J_{HH} = 6.8, CHC′*H*$_3$)[f]	PPh_3 at 135.1 (d, J = 47.0, i), 134.5 (d, J = 10.4, o), 129.6 (d, J = 2.0, p), 128.1 (d, J = 10.1, m); 99.6 (d, J = 2.3, $C_5(CH_3)_5$), 90.6 (d, J = 5.5, OCH), 35.1 (s, CH), 20.2 (s, CH*C*H$_3$), 19.9 (s, CHC′*H*$_3$), 10.5 (s, $C_5(CH_3)_5$)	18.1 (s)
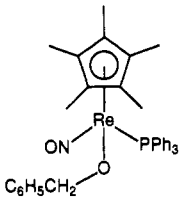 7d	1616 vs (film) 1623 vs (KBr)	7.82–7.73 (m, 6 H of 4 C_6H_5), 7.23–7.14 (m, 4 H of 4 C_6H_5), 7.13–6.94 (m, 10 H of 4 C_6H_5), 5.28 (d, J_{HH} = 13.0, C*H*H′), 5.00 (d, J_{HH} = 13.0, CH*H*′) 1.59 (s, $C_5(CH_3)_5$)	PPh_3 at 134.9 (d, J = 47.3, i), 134.4 (d, J = 10.3, o), 129.7 (d, J = 2.0, p), 128.2 (d, J = 9.4, m); CPh at 148.6 (s, i), 126.5 (s), 125.6 (s);[i] 99.8 (d, J = 2.6, $C_5(CH_3)_5$), 85.5 (d, J = 5.5, CH_2), 10.5 (s, $C_5(CH_3)_5$)	17.2 (s)
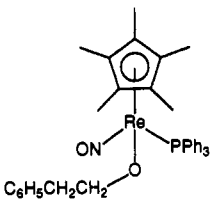 7e	1615 vs (film) 1612 vs (KBr)	7.79–7.69 (m, 6 H of 4 C_6H_5), 7.22–6.96 (m, 14 H of 4 C_6H_5), 4.22 (dd, J_{HH} = 7.6, 5.9, OCH_2),[j] 2.57 (m, C*H*$_2$C$_6$H$_5$), 1.52 (s, $C_5(CH_3)_5$)	PPh_3 at 134.8 (d, J = 47.4, i), 134.6 (d, J = 10.3, o), 129.7 (d, J = 2.0, p), 127.9 (d, J = 10.6, m); CPh at 141.9 (s, i), 129.6 (s), 125.2 (s);[i] 99.7 (d, J = 2.6, $C_5(CH_3)_5$), 84.4 (d, J = 5.7, OCH_2), 44.1 (s, *C*H$_2$C$_6$H$_5$), 10.5 (s, $C_5(CH_3)_5$)	17.6 (s)

[a] Recorded at 300 MHz in CD_2Cl_2 (**5a–e**; referenced to $CDHCl_2$, δ 5.32) or C_6D_6 (**7a–e**; referenced to $Si(CH_3)_4$, δ 0.00) at ambient probe temperature. All couplings (J) are in hertz. [b] Recorded at 75 MHz in CD_2Cl_2 (**5a–e**; referenced to CD_2Cl_2, 53.8 ppm) or C_6D_6 (**7a–e**; referenced to $Si(CH_3)_4$, 0.00 ppm) at ambient probe temperature unless noted. All couplings are in hertz and are to ^{31}P. Assignments of phenyl carbon resonances were made as described in footnote *c* of Table I in: Buhro, W. E.; Georgiou, S.; Fernández, J. M.; Patton, A. T.; Strouse, C. E.; Gladysz, J. A. *Organometallics* **1986**, *5*, 956. [c] Recorded at 32.2 MHz in CD_2Cl_2 (**5a–e**) or C_6D_6 (**7a–e**) at ambient probe temperature and referenced to external 85% H_3PO_4. [d] The ipso carbon resonance is not resolved at ambient temperature. [e] This resonance is taken from a spectrum recorded at −80 °C; the resonance is not observed at ambient temperature. [f] The methine proton resonance is not observed. [g] The para carbon resonance is not resolved at ambient temperature. [h] Distinct methylene proton resonances are found in CD_2Cl_2: 3.70 (dt, J_{HH} = 9.9, 6.1), 3.56 (dt, J_{HH} = 9.3, 6.8). [i] One phenyl resonance is obscured by C_6D_6. [j] Distinct methylene proton resonances are found in CD_2Cl_2: 3.93 (dt, J_{HH} = 9.5, 7.5), 3.78 (m).

plexes,[10] and a σ-*p*-methoxybenzaldehyde complex,[11] these should adopt structures of the types V and VI (eq ii). The former directs the smaller C=O substituent toward the rhenium fragment and should be more stable. Nucleophiles would be expected to attack V and VI from a direction opposite to the bulky PPh_3 ligand. In Scheme III and all other reactions examined to date,[6] the dominant product stereochemistry is consistent with the transition state sketched in V.

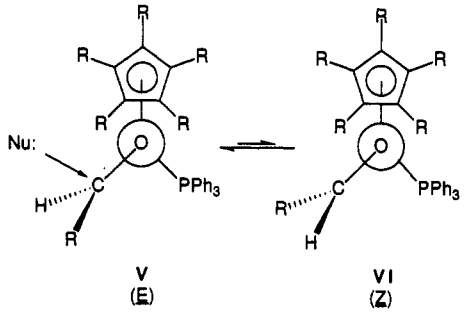

(ii)

Accordingly, diastereoselectivities generally increase as the size differences of the C=O substituents increase. However, the present data clearly indicate that diastereoselection is not a simple function of E/Z isomer equilibrium ratios. Otherwise, the bulkier Lewis acid IV would always give better results than I. Further, small differences should be interpreted with caution. The formyl complex **6** is chiral, and appreciable "double-asymmetric induction" phenomena have been found with cyclopentadienyl complexes **1**.[4] Thus, when both reactants are optically active, one pair of configurations ("matched") gives much better diastereoselectivity than the other ("mismatched"). Additional "nonlinear" effects have also been observed.

3. Conclusion. The structural and chemical properties of pentamethylcyclopentadienyl aldehyde complexes (*RS*,*SR*)-**5** are strikingly similar to those of **1**. The comparable diastereoselectivities found for nucleophilic addition suggest, but by no means require, the intermediacy of σ isomers. Thus, alternative means of probing these reaction coordinates are under investigation. Of these, the most promising is a rate study of cyanide addition to aromatic aldehyde complexes $[(\eta^5\text{-}C_5H_5)Re(NO)(PPh_3)(O{=}CHAr)]^+BF_4^-$.[28] The data unambiguously show that σ isomers are more reactive than π isomers but at the same time reveal other subtleties in the diastereoselection process. These results will be communicated in the near future.

Experimental Section

General Methods. General procedures and purification methods for the solvents and reagents employed in this study have been previously described.[4,17]

(*RS*,*SR*)-[(η^5-C_5Me_5)Re(NO)(PPh_3)(η^2-O=CHCH$_3$)]$^+$BF$_4^-$ ((*RS*,*SR*)-5a). Complex (η^5-C_5Me_5)Re(NO)(PPh_3)(CH_3) (**3**;[16]

(28) Klein, D. P.; Gladysz, J. A. Manuscript in preparation.

Table II. Summary of Crystallographic Data for Propionaldehyde Complex (RS,SR)-[(η^5-C_5Me_5)Re(NO)(PPh_3)(η^2-O=$CHCH_2CH_3$)]$^+BF_4^-$ ((RS,SR)-5b)

molecular formula	$C_{31}H_{36}BF_4NO_2PRe$
molecular weight	758.617
crystal system	monoclinic
space group	$P2_1/c$ (No. 14)
temp of collection, °C	16 (1)
cell dimensions	
a, Å	10.610 (1)
b, Å	21.556 (2)
c, Å	14.244 (1)
β, deg	106.73 (1)
V, Å^3	3119.83
Z	4
d_{obsd}, g/cm^3 (26.5 °C)	1.625
d_{calcd}, g/cm^3	1.615
crystal dimensions, mm	0.30 × 0.25 × 0.20
radiation, Å	λ(Mo Kα), 0.71073
data collection method	$\theta/2\theta$
scan speed, deg/min	variable, 3–8
range/indices (hkl)	0 11, 0 23, −15 +15
scan range	$K_{\alpha1}$ −1.0 to $K_{\alpha2}$ +1.0
total bkgd time/scan time	0.5
no. of reflcns between std	98
total no. of unique data	3150
no. of obsd data, $I > 3\sigma(I)$	3149
abs coeff (μ), cm^{-1}	40.481
min transmissn, %	87
max transmissn, %	99
no. of variables	371
$R = \sum[\lvert\lvert F_o\rvert - \lvert F_c\rvert\rvert]/\sum\lvert F_o\rvert$	0.0294
$R_w = \sum(\lvert\lvert F_o\rvert - \lvert F_c\rvert\rvert)w^{1/2}/\sum\lvert F_o\rvert w^{1/2}$	0.0322
goodness of fit	2.52
$\Delta\rho$(max), e/Å^3	0.902

0.750 g, 1.19 mmol), CH_2Cl_2 (ca. 20 mL), and HBF_4·OEt_2 (169 μL, 1.31 mmol) were combined at −80 °C as previously described to give [(η^5-C_5Me_5)Re(NO)(PPh_3)($ClCH_2Cl$)]$^+BF_4^-$ (**4**).[14] Then acetaldehyde (200 μL, 3.58 mmol) was added with stirring. After 10 min, the cooling bath was removed and the mixture was stirred for an additional 0.5 h. Solvents were then concentrated to ca. 2 mL, and ether (ca. 100 mL) was added. The resulting powder was collected by filtration, washed with ether, and dried under oil pump vacuum to give tan microcrystalline prisms of (RS,SR)-**5a** (0.754 g, 1.01 mmol, 85%), mp 183–185 °C dec. Anal. Calcd for $C_{30}H_{34}BF_4NO_2PRe$: C, 48.39; H, 4.60. Found: C, 48.22; H, 4.61.

(RS,SR)-[(η^5-C_5Me_5)Re(NO)(PPh_3)(η^2-O=$CHCH_2CH_3$)]$^+BF_4^-$ ((RS,SR)-5b). Complex **3** (1.000 g, 1.59 mmol), CH_2Cl_2 (ca. 25 mL), HBF_4·OEt_2 (220 μL, 1.73 mmol), and propionaldehyde (344 μL, 4.77 mmol) were combined in a procedure analogous to that given for (RS,SR)-**5a**. An identical workup gave (RS,SR)-**5b** (1.030 g, 1.36 mmol, 86%) as amber microcrystalline prisms, mp 182–184 °C dec. Anal. Calcd for $C_{31}H_{36}BF_4NO_2PRe$: C, 49.08; H, 4.65. Found: C, 48.95; H, 4.82.

(RS,SR)-[(η^5-C_5Me_5)Re(NO)(PPh_3)(η^2-O=CHCH(CH_3)$_2$)]$^+BF_4^-$ ((RS,SR)-5c). Complex **3** (0.860 g, 1.37 mmol), CH_2Cl_2 (ca. 20 mL), HBF_4·OEt_2 (190 μL, 1.50 mmol), and isobutyraldehyde (234 μL, 4.11 mmol) were combined in a procedure analogous to that given for (RS,SR)-**5a**. An identical workup gave (RS,SR)-**5c** (0.895 g, 1.20 mmol, 88%) as amber microcrystals, mp 166–168 °C dec. Anal. Calcd for $C_{32}H_{38}BF_4NO_2PRe$: C, 49.75; H, 4.96. Found: C, 49.12; H, 4.84.

(RS,SR)-[(η^5-C_5Me_5)Re(NO)(PPh_3)(η^2-O=CHC_6H_5)]$^+BF_4^-$ ((RS,SR)-5d). Complex **3** (0.600 g, 0.954 mmol), CH_2Cl_2 (ca. 15 mL), HBF_4·OEt_2 (132 μL, 1.04 mmol), and benzaldehyde (97 μL, 2.86 mmol) were combined in a procedure analogous to that given for (RS,SR)-**5a**. An identical workup gave (RS,SR)-**5d**·0.5CH_2Cl_2 (0.670 g, 0.809 mmol, 85%) as pink microcrystals, mp 197–198 °C dec. Anal. Calcd for $C_{35}H_{36}BF_4NO_2PRe$·$(CH_2Cl_2)_{0.25}$: C, 51.14; H, 4.44; Cl, 2.14. Found: C, 51.19; H, 4.46; Cl, 2.27.

(RS,SR)-[(η^5-C_5Me_5)Re(NO)(PPh_3)(η^2-O=$CHCH_2C_6H_5$)]$^+BF_4^-$ ((RS,SR)-5e). Complex **3** (0.280 g, 0.445 mmol), CH_2Cl_2 (ca. 10 mL), HBF_4·OEt_2 (63 μL, 0.49 mmol), and phenylacetaldehyde (156 μL, 1.34 mmol) were combined in a procedure analogous to that given for (RS,SR)-**5a**. An identical workup gave (RS,SR)-**5e** (0.324 g, 0.396 mmol, 89%) as tan microcrystals, mp 178–179 °C dec. Anal. Calcd for $C_{36}H_{38}BF_4NO_2PRe$: C, 52.69; H, 4.67. Found: C, 52.45; H, 4.48.

Table III. Atomic Coordinates and Equivalent Isotropic Thermal Parameters of Non-Hydrogen Atoms in (RS,SR)-5b[a]

atom	x	y	z	B (Å^2)
Re	0.17840 (3)	0.11561 (1)	0.23684 (2)	3.937 (6)
P	−0.0473 (2)	0.08817 (9)	0.2332 (1)	3.63 (4)
O1	0.0736 (7)	0.2299 (3)	0.1305 (5)	8.3 (2)
O2	0.1404 (5)	0.0410 (3)	0.1419 (4)	5.9 (1)
N	0.1098 (6)	0.1815 (3)	0.1697 (5)	5.5 (2)
C1	0.2738 (8)	0.0838 (4)	0.4003 (6)	5.0 (2)
C2	0.2598 (7)	0.1496 (4)	0.3947 (6)	5.0 (2)
C3	0.3432 (7)	0.1723 (4)	0.3385 (6)	5.4 (2)
C4	0.4044 (7)	0.1208 (5)	0.3096 (6)	5.7 (2)
C5	0.3606 (8)	0.0663 (4)	0.3463 (6)	5.6 (2)
C6	0.2211 (9)	0.0438 (5)	0.4672 (6)	6.8 (3)
C7	0.1968 (9)	0.1901 (5)	0.4549 (7)	6.9 (3)
C8	0.370 (1)	0.2389 (5)	0.3231 (8)	7.9 (3)
C9	0.5133 (9)	0.1255 (6)	0.2619 (8)	9.2 (3)
C10	0.407 (1)	0.0017 (5)	0.3374 (8)	8.4 (3)
C11	−0.1643 (6)	0.1059 (3)	0.1143 (5)	3.9 (2)
C12	−0.2710 (7)	0.1454 (4)	0.1045 (6)	5.0 (2)
C13	−0.3562 (8)	0.1566 (5)	0.0110 (7)	6.3 (2)
C14	−0.3378 (8)	0.1299 (4)	−0.0715 (6)	5.8 (2)
C15	−0.2330 (9)	0.0915 (5)	−0.0602 (6)	6.5 (2)
C16	−0.1450 (8)	0.0794 (4)	0.0306 (6)	5.5 (2)
C17	−0.0793 (8)	0.0074 (3)	0.2522 (5)	4.4 (2)
C18	−0.2099 (8)	−0.0108 (4)	0.2473 (6)	5.6 (2)
C19	−0.236 (1)	−0.0721 (5)	0.2648 (8)	7.7 (3)
C20	−0.137 (1)	−0.1154 (4)	0.2847 (7)	8.1 (3)
C21	−0.012 (1)	−0.1000 (4)	0.2870 (7)	7.2 (3)
C22	0.0221 (9)	−0.0368 (4)	0.2699 (6)	5.4 (2)
C23	−0.1034 (6)	0.1319 (3)	0.3227 (5)	4.0 (2)
C24	−0.1330 (7)	0.1038 (4)	0.4026 (5)	5.1 (2)
C25	−0.1739 (8)	0.1399 (5)	0.4691 (6)	6.5 (2)
C26	−0.1843 (9)	0.2025 (5)	0.4591 (6)	7.1 (3)
C27	−0.1540 (9)	0.2313 (4)	0.3810 (7)	6.7 (2)
C28	−0.1120 (8)	0.1970 (4)	0.3123 (6)	5.3 (2)
C29	0.2350 (9)	0.0718 (5)	0.1184 (6)	7.1 (3)
C30	0.204 (1)	0.1019 (7)	0.0187 (8)	11.3 (4)
C31	0.295 (1)	0.134 (1)	−0.000 (1)	17.4 (6)

[a] Atoms refined anisotropically are given in the form of the isotropic equivalent displacement parameter, defined as $^4/_3[a^2B(1,1) + b^2B(2,2) + c^2B(3,3) + ab(\cos\gamma)B(1,2) + ac(\cos\beta)B(1,3) + bc(\cos\alpha)B(2,3)]$.

Table IV. Selected Bond Lengths (Å) and Angles (deg) in (RS,SR)-5b

Re–P	2.453 (1)	Re–C5	2.359 (5)
Re–N	1.751 (5)	C1–C2	1.426 (7)
N–O1	1.193 (7)	C1–C5	1.411 (8)
Re–O2	2.066 (4)	C1–C6	1.507 (9)
Re–C29	2.163 (7)	C2–C3	1.439 (8)
C29–O2	1.325 (7)	C2–C7	1.509 (9)
C29–C30	1.51 (1)	C3–C4	1.41 (1)
C30–C31	1.28 (2)	C3–C8	1.492 (8)
Re–C1	2.358 (5)	C4–C5	1.417 (9)
Re–C2	2.285 (5)	C4–C9	1.503 (8)
Re–C3	2.278 (5)	C5–C10	1.49 (1)
Re–C4	2.324 (5)		
P–Re–N	86.2 (2)	C5–C1–C6	127.6 (5)
Re–N–O1	173.0 (4)	C1–C2–C3	107.4 (5)
P–Re–C29	111.5 (2)	C1–C2–C7	126.8 (5)
N–Re–C29	95.4 (3)	C3–C2–C7	124.3 (5)
P–Re–O2	78.1 (1)	C2–C3–C4	107.7 (5)
N–Re–O2	107.6 (2)	C2–C3–C8	125.8 (6)
O2–Re–C29	36.4 (2)	C4–C3–C8	126.3 (5)
Re–O2–C29	75.8 (3)	C3–C4–C5	108.6 (5)
Re–C29–O2	67.8 (3)	C3–C4–C9	123.9 (6)
Re–C29–C30	120.9 (6)	C5–C4–C9	126.8 (6)
O2–C29–C30	118.6 (6)	C4–C5–C10	126.1 (6)
C29–C30–C31	117.3 (9)	C1–C5–C4	108.3 (5)
C2–C1–C5	108.0 (5)	C1–C5–C10	125.4 (5)
C2–C1–C6	123.7 (5)		

Optically Active Aldehyde Complexes. A. Complex (+)-(*S*)-**3**[19] was dissolved in CH_2Cl_2 and treated with $HBF_4 \cdot OEt_2$ and aldehydes in procedures analogous to the above. The products (+)-(*RS*)-**5** were not analytically pure. Selected data: (+)-(*RS*)-**5a** (89%) $[\alpha]^{26}_{589}$ 67 ° (*c* 0.44 mg/mL, $CHCl_3$); (+)-(*RS*)-**5d** (53–89%) $[\alpha]^{26}_{589}$ 216–282° (*c* 0.33–0.38 mg/mL, $CHCl_3$ or CH_2Cl_2).

B. A Schlenk flask was charged with (+)-(*S*)-**3** (0.101 g, 0.161 mmol), C_6H_5Cl (8 mL), and a stir bar. The solution was cooled to −45 °C, and $HBF_4 \cdot OEt_2$ (25 μL, 0.198 mmol) was added with stirring. After 15 min, isobutyraldehyde (73 μL, 0.804 mmol) was added. After 15 min, the cooling bath was removed and the mixture was stirred for 20 min. The solution was added dropwise to a rapidly stirred mixture of ether (50 mL) and hexane (25 mL). The precipitate was collected by filtration and dried under oil pump vaccum to give (+)-(*RS*)-**5c** (0.094 g, 0.122 mmol, 76%) as a tan powder: mp 156–160 °C dec; $[\alpha]^{25}_{589}$ 112° (*c* 0.34 mg/mL, CH_2Cl_2). Anal. Calcd for $C_{32}H_{38}BF_4NO_2PRe$: C, 49.75; H, 4.96. Found: C, 49.24; H, 4.34.

(η^5-C_5Me_5)Re(NO)(PPh_3)(OCH_2CH_3) (7a). A Schlenk flask was charged with (*RS*,*SR*)-**5a** (0.177 g, 0.238 mmol), a stir bar, and CH_2Cl_2 (10 mL). The amber solution was cooled to −80 °C, and (η^5-C_5H_5)Re(NO)(PPh_3)(CHO) (**6**;[21] 0.136 g, 0.238 mmol) was added as a solid. The resulting suspension was stirred. After 10 min, the cooling bath was removed, and the mixture was stirred for an additional 15 min. Solvent was removed under oil pump vacuum, and the residue was extracted with benzene (3 × 5 mL). The insoluble material was collected by filtration and washed with benzene to give [(η^5-C_5H_5)Re(NO)(PPh_3)(CO)]$^+BF_4^-$ (**8**; 0.149 g, 0.226 mmol, 95%).[21] The extracts were passed via cannula through a 1 × 4 cm column of deactivated Florisil in a Kramer filter.[29] Solvent was removed from the eluate under oil pump vacuum to give an orange-brown foam/oil, which was dissolved in ether (2 mL). Solvent was removed under oil pump vacuum to give **7a** as an orange-brown foam (0.133 g, 0.202 mmol, 85%), mp 63–65 °C dec. Anal. Calcd for $C_{30}H_{35}NO_2PRe$: C, 54.70; H, 5.35; N, 2.13. Found: C, 54.56; H, 5.39; N, 2.08.

(η^5-C_5Me_5)Re(NO)(PPh_3)($OCH_2CH_2CH_3$) (7b). Complex (*RS*,*SR*)-**5b** (0.218 g, 0.287 mmol), **6** (0.164 g, 0.287 mmol), and CH_2Cl_2 (10 mL) were combined in a procedure analogous to that given for **7a**. An identical workup gave **8** (0.178 g, 0.270 mmol, 94%) and **7b** as a dark orange foam (0.170 g, 0.253 mmol, 88%), mp 138–140 °C dec. Anal. Calcd for $C_{31}H_{37}NO_2PRe$: C, 55.34; H, 5.54; N, 2.08. Found: C, 55.25, H, 5.56, N, 2.05.

(η^5-C_5Me_5)Re(NO)(PPh_3)($OCH_2CH(CH_3)_2$) (7c). Complex (*RS*,*SR*)-**5c** (0.158 g, 0.204 mmol), **6** (0.117 g, 0.204 mmol), and CH_2Cl_2 (10 mL) were combined in a procedure analogous to that given for **7a**. An identical workup gave **7c** as an orange-brown foam (0.110 g, 0.160 mmol, 79%), mp 57.5–59 °C dec. Anal. Calcd for $C_{32}H_{39}NO_2PRe$: C, 55.96; H, 5.72. Found: C, 55.24; H, 5.59.

(η^5-C_5Me_5)Re(NO)(PPh_3)($OCH_2C_6H_5$) (7d). Complex (*RS*,*SR*)-**5d** (0.226 g, 0.280 mmol), **6** (0.160 g, 0.280 mmol), and CH_2Cl_2 (10 mL) were combined in a procedure analogous to that given for **7a**. An identical workup gave **7d** as an orange-brown foam (0.176 g, 0.244 mmol, 87%), mp 164–166 °C dec. Anal. Calcd for $C_{35}H_{37}NO_2PRe$: C, 58.32; H, 5.17; N, 1.94. Found: C, 58.39; H, 5.20; N, 1.90.

(η^5-C_5Me_5)Re(NO)(PPh_3)($OCH_2CH_2C_6H_5$) (7e). Complex (*RS*,*SR*)-**5e** (0.134 g, 0.163 mmol), **6** (0.094 g, 0.163 mmol), and CH_2Cl_2 (10 mL) were combined in a procedure analogous to that given for **7a**. An identical workup gave **7e** as an orange-brown foam (0.098 g, 0.134 mmol, 82%), mp 58–60 °C dec. Anal. Calcd for $C_{36}H_{39}NO_2PRe$: C, 58.84; H, 5.35. Found: C, 58.34; H, 5.31.

Deuterated Alkoxide Complexes (η^5-C_5Me_5)Re(NO)(PPh_3)(OCHDR) (7-d_1). The following is representative. A 5-mm NMR tube was charged with (*RS*,*SR*)-**5a** (0.039 g, 0.052 mmol) and (η^5-C_5H_5)Re(NO)(PPh_3)(CDO) (**6**-d_1; 0.030 g, 0.052 mmol)[4] and was capped with a septum. The tube was placed in liquid nitrogen, and CD_2Cl_2 (ca. 0.7 mL) was added by syringe. The mixture was degassed through two freeze–pump–thaw cycles. The tube was warmed to −80 °C and transferred to a −80 °C NMR probe. The probe was slowly warmed to 30 °C, and ^1H NMR spectra were recorded at 5–10 °C intervals. Data: Scheme III and Figure 4.

Crystal Structure of (*RS*,*SR*)-5b. Ether vapor was allowed to slowly diffuse into a CH_2Cl_2 solution of (*RS*,*SR*)-**5b**. An amber crystal was mounted on a glass fiber for preliminary data collection on a Syntex P$\bar{1}$ diffractometer. Cell constants (Table I) were obtained from 15 centered reflections with 20° < 2θ < 30°. Lorentz and polarization corrections and an empirical absorption correction based upon a series of Ψ scans were applied to the data. The structure was solved by standard heavy-atom techniques using the SDP/VAX package.[30] All non-hydrogen atoms were refined with anisotropic thermal parameters. Hydrogen atom positions were calculated and not refined. Scattering factors and Δ*f*′ and Δ*f*″ values were taken from the literature.[31] Anomalous dispersion effects were included in F_c.[32]

Acknowledgment. We thank the NIH for support of this research and the Centre National de la Recherche Scientifique from France and Organisation des Traités de l'Atlantique Nord for a fellowship (F.A.).

Supplementary Material Available: A table of anisotropic thermal parameters for (*RS*,*SR*)-**5b** (1 page); a listing of observed and calculated structure factors (11 pages). Ordering information is given on any current masthead page.

(29) Brown, H. C. *Organic Syntheses via Boranes*; Wiley: New York, 1975; Figure 9.26; Aldrich Catalog No. Z10,139-7.

(30) Frenz, B. A. The Enraf-Nonius CAD 4 SDP -- A Real-time System for Concurrent X-ray Data Collection and Crystal Structure Determination. In *Computing and Crystallography*; Schenk, H., Olthof-Hazelkamp, R., van Konigsveld, H., Bassi, G. C., Eds.; Delft University Press: Delft, Holland, 1978; pp 64–71.

(31) Cromer, D. T.; Waber, J. T. In *International Tables for X-ray Crystallography*; Ibers, J. A., Hamilton, W. C., Eds.; Kynoch: Birmingham, England, 1974; Vol. IV, pp 72–98, 149–150, Tables 2.2B and 2.3.1.

(32) Ibers, J. A.; Hamilton, W. C. *Acta Crystallogr.* **1964**, *17*, 781.